

## **General Disclaimer**

### **One or more of the Following Statements may affect this Document**

- This document has been reproduced from the best copy furnished by the organizational source. It is being released in the interest of making available as much information as possible.
- This document may contain data, which exceeds the sheet parameters. It was furnished in this condition by the organizational source and is the best copy available.
- This document may contain tone-on-tone or color graphs, charts and/or pictures, which have been reproduced in black and white.
- This document is paginated as submitted by the original source.
- Portions of this document are not fully legible due to the historical nature of some of the material. However, it is the best reproduction available from the original submission.

**CALCULATION OF TURBULENT SHEAR STRESS IN SUPERSONIC  
BOUNDARY LAYER FLOWS**

by

**Chen-Chih Sun\***

and

**Morris E. Childs<sup>+</sup>**

**University of Washington, Seattle, Washington**

**Index Categories: Boundary Layers and Convective Heat Transfer -  
Turbulent; Supersonic and Hypersonic Flow;  
Shock Waves**

**(NASA-CR-138302) CALCULATION OF TURBULENT  
SHEAR STRESS IN SUPERSONIC BOUNDARY LAYER  
FLOWS (Washington Univ.) 15 p HC \$4.00**

**CSCL 20D**

**G3/12**



**\* Research Assistant Professor, Department of Mechanical Engineering,  
University of Washington, Seattle, Washington. Member AIAA.**

**+ Professor and Chairman, Department of Mechanical Engineering,  
University of Washington, Seattle, Washington. Member AIAA.**

**This work was supported by NASA Grant NGR-48-002-047 under administration  
of the Aerodynamics Branch, Ames Research Center.**

## SYMBOLS

$C_f$	= skin friction coefficient
$M$	= Mach number
$P$	= pressure
$r$	= distance normal to centerline
$R$	= radius of the duct
$T_{ij}$	= total stress tensor
$u$	= time averaged velocity in primary flow direction
$v$	= time averaged velocity normal to centerline
$x$	= distance parallel to centerline
$y$	= $R-r$
$\delta$	= boundary layer thickness
$\mu$	= molecular viscosity
$\eta$	= $y/\delta$
$\rho$	= time averaged density
$\tau$	= shear stress

## Subscripts

$e$	= boundary layer edge condition
$\infty$	= free stream condition

## Superscript

$\langle ( )' \rangle$	= time averaged fluctuation value
------------------------	-----------------------------------

PRECEDING PAGE BLANK NOT FILMED

## INTRODUCTION

In the study of supersonic turbulent boundary layer flow the turbulent shear stress distribution has always been of great importance and interest. The direct measurement of the turbulent shear stress is, however, quite difficult. A natural alternative is to compute the shear from experimental mean flow data by numerically integrating the momentum equation. Such computations have been performed in recent studies by Bushnell and Morris<sup>1</sup>, Horstman and Owen<sup>2</sup>, and Sturek<sup>3</sup>. This note describes results obtained by a computational procedure which differs from those previously reported in that integrated mass and momentum flux profiles and differentials of these integral quantities are used in the computations so that local evaluation of the streamwise velocity gradient is not necessary. The computed results are compared with measured shear stress data obtained by using hot wire anemometer and laser velocimeter techniques in recent studies by Rose and Johnson<sup>4,5</sup>. The measurements of Rose and Johnson were made upstream and downstream of an adiabatic unseparated interaction of an oblique shock wave with the turbulent boundary layer on the flat wall of a two-dimensional,  $M_\infty = 2.9$  wind tunnel. The shock wave was generated by a  $7^\circ$  wedge. The turbulence data obtained from the two independent systems of measurement were in reasonably good agreement, indicating that the data should be reliable. The computational procedure developed here is easy to use and the computed results show reasonably good overall agreement with those obtained by direct measurement. As would be expected for any method of computing shear stress from mean flow data, the computed values of shear stress are quite sensitive to small differences in mean flow profiles and to simplifying assumptions which may be made in developing the relationships to be used in the computations. The effect of some of these differences on computed shear stress distributions is discussed.

## BASIC EQUATIONS AND BOUNDARY CONDITIONS

The time-averaged equations for the conservation of mass and momentum for steady compressible turbulent boundary layer flow in an axisymmetric channel are, respectively,

$$\frac{\partial}{\partial x} (\rho u) + \frac{\partial}{\partial x} \langle \rho' u' \rangle + \frac{1}{r} \frac{\partial}{\partial r} (r \rho v) + \frac{1}{r} \frac{\partial}{\partial r} (r \langle \rho' v' \rangle) = 0 \quad (1)$$

and

$$\frac{\partial}{\partial x} (\rho u^2) + \frac{1}{r} \frac{\partial}{\partial r} (r \rho u v) = - \frac{\partial \tau}{\partial x} + \frac{\partial}{\partial x} T_{xx} + \frac{1}{r} \frac{\partial}{\partial r} T_{rx} \quad (2)$$

where

$$T_{xx} = (\tau_v)_{xx} - (\rho \langle u'^2 \rangle + 2u \langle \rho' u' \rangle) \quad (3)$$

$$T_{rx} = (\tau_v)_{rx} - (\rho \langle u' v' \rangle + u \langle \rho' v' \rangle + v \langle \rho' u' \rangle) \quad (4)$$

with  $\tau_v$  representing the viscous stress.

If we assume that  $|v \langle \rho' u' \rangle| \ll |\rho \langle u' v' \rangle|$  and  $|\frac{\partial}{\partial x} \langle \rho' u' \rangle| \ll |\frac{\partial}{\partial x} (\rho u)|$  and transform to an x-y coordinate system, the continuity and momentum equations may be combined and integrated in a direction normal to the surface to yield

$$\begin{aligned} \frac{\tau}{\rho_e u_e^2} (1 - \eta \frac{\delta}{R}) &= \frac{C_f}{2} + \left( \frac{d\delta}{dx} + \frac{\delta}{\rho_e u_e^2} \frac{d\rho_e u_e^2}{dx} + \frac{\delta}{R} \frac{dR}{dx} \right) \int_0^\eta \frac{\rho u^2}{\rho_e u_e^2} d\eta \\ &- \left( \frac{2\delta}{R} \frac{d\delta}{dx} + \frac{\delta^2}{\rho_e u_e^2 R} \frac{d\rho_e u_e^2}{dx} \right) \int_0^\eta \frac{\rho u^2}{\rho_e u_e^2} d\eta \\ &- \left( \frac{d\delta}{dx} + \frac{\delta}{R} \frac{dR}{dx} + \frac{\delta}{\rho_e u_e} \frac{d\rho_e u_e}{dx} \right) \frac{u}{u_e} \int_0^\eta \frac{\rho u}{\rho_e u_e} d\eta \\ &+ \left( \frac{2\delta}{R} \frac{d\delta}{dx} + \frac{\delta^2}{\rho_e u_e R} \frac{d\rho_e u_e}{dx} \right) \frac{u}{u_e} \int_0^\eta \eta \frac{\rho u}{\rho_e u_e} d\eta \end{aligned}$$

$$\begin{aligned}
& + \frac{\delta}{\rho_e u_e^2 R} \int_0^\eta (R - \eta \delta) \left( \frac{dp}{dx} - \frac{d}{dx} T_{xx} \right) d\eta \\
& + \delta \frac{\partial}{\partial x} \int_0^\eta \frac{\rho u^2}{\rho_e u_e^2} d\eta - \frac{\delta^2}{R} \frac{\partial}{\partial x} \int_0^\eta \eta \frac{\rho u^2}{\rho_e u_e^2} d\eta \\
& - \delta \frac{u}{u_e} \frac{\partial}{\partial x} \int_0^\eta \frac{\rho u}{\rho_e u_e} d\eta + \frac{u}{u_e} \frac{\delta^2}{R} \frac{\partial}{\partial x} \int_0^\eta \eta \frac{\rho u}{\rho_e u_e} d\eta
\end{aligned} \tag{5}$$

where  $\tau = \mu \frac{\partial u}{\partial y} - \rho \langle u'v' \rangle$ .

Equation (5) becomes applicable to two-dimensional flow as  $R \rightarrow \infty$ .

The normal stress,  $T_{xx}$ , which appears in equation (5), is not known from mean profile data. However, computations which have been made in this study show that its effect is small. In the results shown, the streamwise gradient of  $T_{xx}$  has been neglected.

Knowledge is also required of the static pressure distribution in the boundary layer. In many studies of supersonic boundary layer flow no attempt is made to measure the static pressure variation normal to the wall, even though, for some adverse pressure gradient flows, the variation may, in fact, be rather large. In most instances the static pressure at the boundary layer edge may be determined with confidence. If this is done, the normal pressure variation may then be represented in approximate fashion by assuming a linear distribution between the wall static pressure and the pressure at the boundary layer edge. Results are shown here for both a linear static pressure distribution and a constant static pressure.

Examination of equation (5) shows that an accurate value of boundary layer growth rate is very important for the calculation of the shear stress. However, precise determination of the boundary layer thickness from experimental mean data is difficult. It is even more difficult to evaluate the boundary layer growth rate accurately. This problem may be avoided by using the condition that the

shear stress diminishes to zero at the boundary layer edge and solving equation (5) for  $d\delta/dx$ :

$$\begin{aligned}
 \frac{d\delta}{dx} = & \left[ \frac{C_f}{2} + \left( \frac{\delta}{\rho_e u_e^2} \frac{d\rho_e u_e^2}{dx} + \frac{\delta}{R} \frac{dR}{dx} \right) \int_0^1 \frac{\rho u^2}{\rho_e u_e^2} d\eta - \frac{\delta^2}{\rho_e u_e^2 R} \frac{d\rho_e u_e^2}{dx} \int_0^1 \eta \frac{\rho u^2}{\rho_e u_e^2} d\eta \right. \\
 & - \left( \frac{\delta}{R} \frac{dR}{dx} + \frac{\delta}{\rho_e u_e} \frac{d\rho_e u_e}{dx} \right) \int_0^1 \frac{\rho u}{\rho_e u_e} d\eta + \frac{\delta^2}{\rho_e u_e R} \frac{d\rho_e u_e}{dx} \int_0^1 \eta \frac{\rho u}{\rho_e u_e} d\eta \\
 & + \delta \frac{\partial}{\partial x} \int_0^1 \frac{\rho u^2}{\rho_e u_e^2} d\eta - \frac{\delta^2}{R} \frac{\partial}{\partial x} \int_0^1 \eta \frac{\rho u^2}{\rho_e u_e^2} d\eta - \delta \frac{\partial}{\partial x} \int_0^1 \frac{\rho u}{\rho_e u_e} d\eta \\
 & + \frac{\delta^2}{R} \frac{\partial}{\partial x} \int_0^1 \eta \frac{\rho u}{\rho_e u_e} d\eta + \frac{\delta}{\rho_e u_e^2} \frac{dP_w}{dx} \left( 1 - \frac{\delta}{2R} \right) \\
 & + \frac{\delta}{\rho_e u_e^2} \frac{d(P_e - P_w)}{dx} \left( \frac{1}{2} - \frac{\delta}{3R} \right) \left. \right] / \left[ \frac{2\delta}{R} \int_0^1 \eta \frac{\rho u}{\rho_e u_e} d\eta - \int_0^1 \frac{\rho u^2}{\rho_e u_e^2} d\eta \right. \\
 & \left. + \int_0^1 \frac{\rho u}{\rho_e u_e} d\eta - \frac{2\delta}{R} \int_0^1 \eta \frac{\rho u}{\rho_e u_e} d\eta + \frac{(P_e - P_w)}{\rho_e u_e^2} \left( \frac{1}{2} - \frac{\delta}{3R} \right) \right] \quad (6)
 \end{aligned}$$

In equation (6) a linear pressure variation normal to the wall has been assumed.

If the streamwise gradient of the normal stress is ignored and if the flow is assumed to be locally similar, equation (5) reduces to the expression used by Bushnell and Morris<sup>1</sup> in their computation of shear stress.

Before solving for the shear stress from equation (5), it is also necessary to know the coefficient of skin friction. This may be obtained by using the wall-wake velocity profile proposed by Sun and Childs<sup>6</sup>. The method of least-squares may be used to fit the wall-wake profile to the experimental mean velocity profiles to provide values of  $C_f$  and to provide a smoothed representation of the mean velocity distribution.

## RESULTS

In carrying out the computations for the flow downstream of the shock wave-

boundary layer interactions, the departure from local similarity has been taken into account. For purposes of comparison, however, computations based on local similarity have also been made. The effect of static pressure variation normal to the wall has also been considered for the downstream stations by assuming a linear variation in pressure. In these computations the static pressure at the boundary layer edge has been computed from the free stream total pressure and pitot pressure, with appropriate allowance made for the loss in total pressure across the shock system. The velocity and density profiles needed for the computations were obtained from mean flow pitot profiles with appropriate allowance made for static pressure variation across the boundary layer, and under the assumption of constant total temperature across the boundary layer. As was mentioned in the previous section, the mean velocity profiles may be smoothed by using a least squares fit of the wall-wake velocity profile to the experimental profiles. Computations have been made for both smoothed and unsmoothed profiles.

Figure 1 shows shear stress distributions computed for an upstream ( $x = 5.375$  cm) station in Johnson's and Rose's investigation, along with their shear stress data from the hot-wire anemometer and the laser velocimeter measurements. The computed shear values which are shown have been obtained under the assumption of local similarity. As is shown, the calculated results agree quite well over much of the boundary layer, with the measured results obtained with the laser velocimeter. The differences between the calculated results and the hot-wire results are greater. For both the hot-wire and laser velocimeter measurements the peak values of shear stress are seen to occur substantially farther from the wall than is observed for the calculated distributions. Also shown in the figure are values of the wall shear stress as determined by a least squares fit of the wall-wake profile to the mean data and as measured by a Preston tube. The agreement between the two shear stress values is good.

For purposes of comparison, a wall-wake profile proposed earlier by Maise and McDonald<sup>7</sup> has been used to represent the velocity profiles obtained by Rose and Johnson. As is shown, the shear values computed from the Maise-McDonald profile are substantially lower than those obtained with the unsmoothed data or the wall-wake representation described in Reference 6.

Results of the computations for the data of Rose and Johnson for a station downstream of the shock wave-boundary layer interaction ( $x = 9.375$  cm) are shown in Figure 2, along with their measured shear stress distributions. Several sets of computations have been made from the mean data, including one, for purposes of comparison, in which local similarity has been assumed. Results have been obtained for both smoothed and unsmoothed profiles and for both linear and constant static pressure distribution across the boundary layer. The velocity and density profiles used in computing the shear stress are shown in Figure 3, along with the wall-wake representations of the velocity profiles.

As is shown in Figure 2, the measured shear stress values obtained by the two experimental techniques are in quite good agreement. These in turn agree reasonably well with the computed values obtained by using smoothed nonsimilar profiles and the assumption of a linear pressure variation across the boundary layer. There is considerable difference between the results for the smoothed and unsmoothed profiles, with the peak shear stress value for the unsmoothed profile occurring lower in the boundary layer. Near the wall the difference apparently was due primarily to inaccuracy in the numerical integration process for the unsmoothed data. Much smaller step sizes could be used with the smoothed data. The results obtained from the wall-wake profiles are valid, of course, only if the profiles provide accurate representations of the actual velocity distributions. In the outer part of the boundary layer the wall-wake profile provided an excellent representation of the data at one station but did not fit so well at

the other. This would account for some of the difference in computed shear stress for smoothed and unsmoothed profiles in that region.

The computed shear values are quite sensitive to the assumptions regarding static pressure. The computed values of static pressure at the boundary layer edge at the first and second measuring stations differed from those at the wall by 3.0 and 1.2 percent, respectively. As is shown, the computed values of shear stress with no consideration given to the pressure difference across the boundary layer were substantially lower than those obtained when the pressure difference was considered.

As is also shown in Figure 2, the results obtained under the assumption of local similarity are markedly different from those determined when similarity is not assumed. The peak shear stress levels computed assuming local similarity are less than half the values computed when similarity is not assumed. Furthermore, the shapes of the shear stress distribution curves are quite different. These results occur even though the differences between profiles at two closely spaced stations are small. The density and velocity profiles in Figure 3 were obtained at streamwise stations located approximately one boundary layer thickness apart. Although the profiles at successive stations appear at first glance to be quite similar, striking differences are found for the computed shear stress distributions.

#### CONCLUSIONS

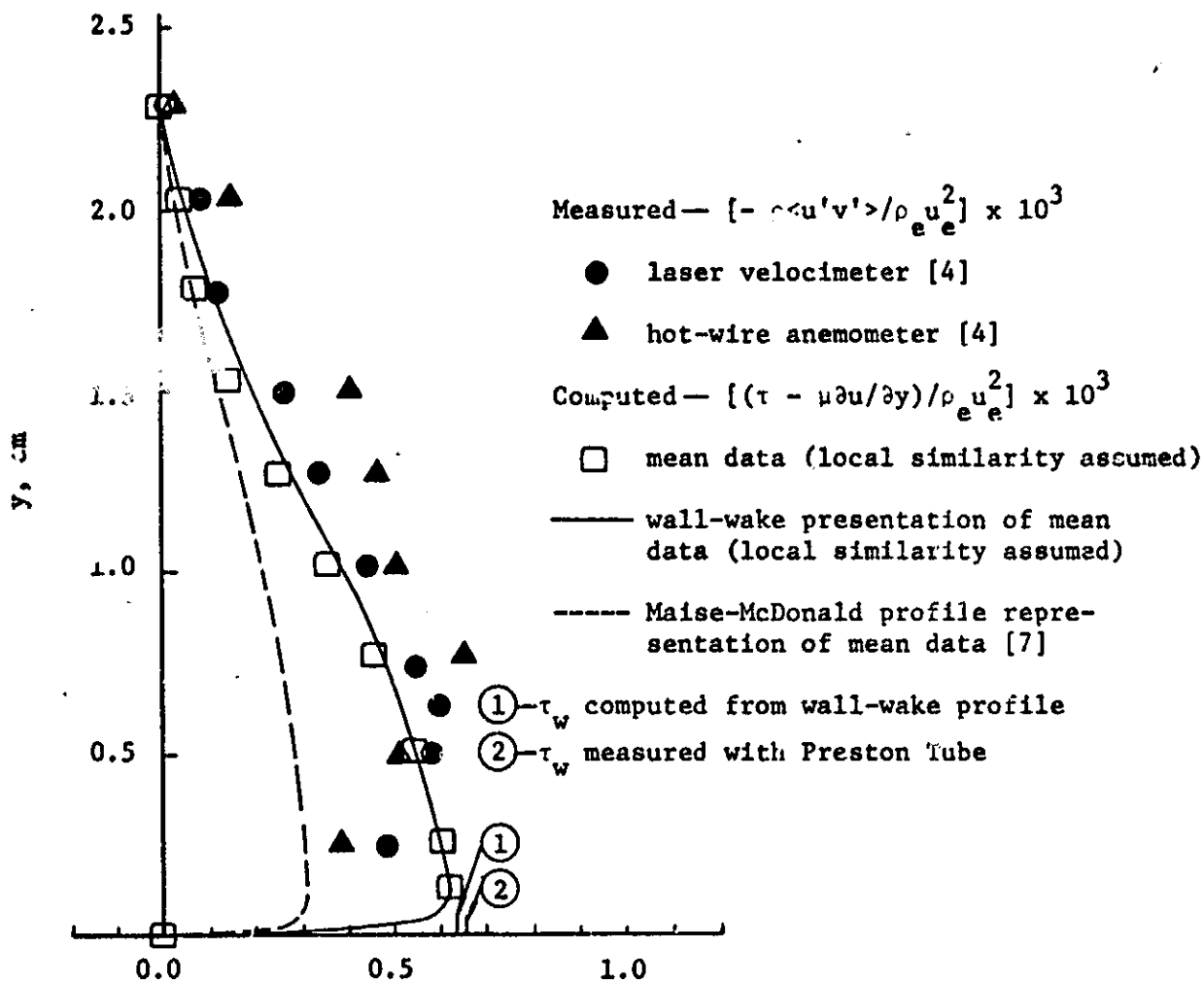
An alternative method of computing shear stress distribution from experimental mean profile data in compressible turbulent boundary layer flow has been developed. The method is different from those previously reported in that integrated mass and momentum flux profiles and differentials of these integral quantities are used in the computations so that a full evaluation of the streamwise velocity gradient is not necessary. The method has been found to yield results which are in very good overall agreement with directly measured

turbulence data for two-dimensional adiabatic boundary layer flow in the regions upstream and downstream of an oblique shock wave interaction. The computed results are quite sensitive to the accuracy of the numerical integrations required in the computational procedure and to the mean property distributions in the boundary layer. The assumption of local similarity may cause large errors in computed shear stress values for flows subjected to pressure gradients, even though adjacent profiles of the mean properties may appear, on first examination, to be quite similar. The computed shear stress levels are quite sensitive to the static pressure distribution normal to the wall. Thus, if reliable shear stress distributions are to be obtained from mean profile data, the static pressure distribution must be known rather accurately. The effect of the streamwise gradient of the normal stress on the computed results is small and apparently may be neglected.

## REFERENCES

1. Bushnell, D.M. and Morris, D.J., "Shear-Stress, Eddy-Viscosity and Mixing Length Distributions in Hypersonic Turbulent Boundary Layers," NASA TMX-2310, 1971.
2. Horstman, C.C. and Owen, F.K., "Turbulent Properties of a Compressible Boundary Layer," AIAA Journal, vol. 10, no. 11, November 1972, pp. 1418-1424.
3. Sturek, W.B., "Calculations of Turbulent Shear Stress in Supersonic Turbulent Boundary Layer Zero and Adverse Pressure Gradient Flow," AIAA Paper No. 73-166, January 1973.
4. Johnson, D.A. and Rose, W.C., "Measurement of Turbulent Transport Properties in a Supersonic Boundary-Layer Flow Using Laser Velocimeter and Hot Wire Anemometer Techniques," AIAA Paper 73-1045, Seattle, Washington, 1973.
5. Rose, W.C. and Johnson, D.A., "A Study of Shock Wave Turbulent Boundary Layer Interaction Using Laser Velocimeter and Hot Wire Anemometer Techniques," AIAA Paper 74-95, Washington, D.C., 1974.
6. Sun, C.C. and Childs, M.E., "A Modified Wall-Wake Velocity Profile for Turbulent Compressible Boundary Layers," Journal of Aircraft, vol. 10, no. 6, June 1973, pp. 381-383.
7. Maise, G. and McDonald, H., "Mixing Length and Kinematic Eddy Viscosity in a Compressible Boundary Layer," AIAA Journal, vol. 6, no. 1, January 1968, pp. 73-80.

- Figure 1. Turbulent shear stress distribution upstream of a shock wave-boundary layer interaction, two-dimensional tunnel [4]
- Figure 2. Turbulent shear stress distribution downstream of a shock wave-boundary layer interaction, two-dimensional tunnel [5]
- Figure 3. Density and velocity profiles downstream of a shock wave-boundary layer interaction [5]



$$[-\rho \langle u'v' \rangle / \rho_e u_e^2] \times 10^3, \quad [(\tau - \mu \partial u / \partial y) / \rho_e u_e^2] \times 10^3$$

